



Contents lists available at ScienceDirect

Journal of the Mechanics and Physics of Solids

journal homepage: www.elsevier.com/locate/jmps

An arterial constitutive model accounting for collagen content and cross-linking

Gerhard A. Holzapfel^{a,b,*}, Ray W. Ogden^c^aInstitute of Biomechanics, Graz University of Technology, Stremayrgasse 16-II, Graz 8010, Austria^bNorwegian University of Science and Technology (NTNU), Department of Structural Engineering, Trondheim 7491, Norway^cSchool of Mathematics and Statistics, University of Glasgow, University Place, Glasgow G12 8SQ, Scotland, UK

ARTICLE INFO

Article history:

Received 22 June 2019

Revised 8 August 2019

Accepted 8 August 2019

Available online xxx

Keywords:

Artery elasticity

Collagen fibers

Collagen cross-links

Fibrous tissue

ABSTRACT

It is apparent from the literature that the density of cross-links in collagenous tissue has a stiffening effect on the mechanical response of the tissue. This paper represents an initial attempt to characterize this effect on the elastic response, specifically in respect of arterial tissue. Two approaches are presented. First, a simple phenomenological continuum model with a cross-link-dependent stiffness is considered, and the influence of the cross-link density on the response in uniaxial tension is illustrated. In the second approach, a 3D model is developed that accounts for the relative orientation and stiffness of (two families of) collagen fibers and cross-links and their coupling using an invariant-based strain-energy function. This is also illustrated for uniaxial tension, and the influence of different cross-link arrangements and material parameters is detailed. Specialization of the model for plane strain is then used to show the effect of the cross-link orientation (relative to the fibers) and cross-link density on the shear stress versus the amount of shear deformation response. The elasticity tensor for the general (3D) case is provided with a view to subsequent finite element implementation.

© 2019 The Authors. Published by Elsevier Ltd.
This is an open access article under the CC BY license.
(<http://creativecommons.org/licenses/by/4.0/>)

1. Introduction

Collagen is the most important structural protein in the body and is able to bear significant mechanical load within fibrous tissues (Fratzl, 2008). In such tissues collagen forms a network together with cross-links which, from the solid mechanics point of view, contribute to the transmission of forces between the fibers of the network in both healthy and aged tissues (Andriotis et al., 2018). Collagen is a hierarchical material (Fratzl, 2008; Fratzl and Weinkamer, 2007), which is composed of a tropocollagen triple helix at the nanoscale, typically about 300 nm long. This tropocollagen is held together by intramolecular bonds. Aggregates of tropocollagen molecules connected together by cross-links form collagen fibrils which themselves group together to form collagen fibers. Enzymatic cross-links, which connect tropocollagen molecules at their ends and provide stability of the structure, contribute to the mechanical resistance of a fibril under tension. On the other hand non-enzymatic cross-links which can attach at any point along the length of a tropocollagen molecule can be

* Corresponding author.

E-mail address: holzapel@tugraz.at (G.A. Holzapfel).

<https://doi.org/10.1016/j.jmps.2019.103682>

0022-5096/© 2019 The Authors. Published by Elsevier Ltd. This is an open access article under the CC BY license.

(<http://creativecommons.org/licenses/by/4.0/>)

detrimental to normal fibril function. The bonds may occur as bivalent and/or trivalent cross-links (Eekhoff et al., 2018). Under suitable loads bonds can be broken, and sliding between the filaments may occur.

Clearly, cross-linking of collagen fibers has a significant effect on the response of the tissues within which the fibers are embedded (Buehler, 2008; Eekhoff et al., 2018; Yoshida et al., 2014); the influence of cross-links on the fracture mechanics of collagen fibrils is documented in Svensson et al. (2013). There is a lot of evidence, however, that indicates that the number of cross-links increases with age, which is an important factor in the age-related stiffening of arterial walls (Barodka et al., 2011; Cantini et al., 2001). However, there is a lack of quantitative data concerning age-related changes of cross-linking in biological tissues (Hayashi and Hirayama, 2017). On the basis of bovine tail tendons the study of Willett et al. (2010) found that aged tissues contain more mature covalent cross-links. According to the review article of Tsamis et al. (2013) there are two different mechanisms responsible for the increase of cross-links: (i) increase of the amount of cross-linking amino acids within collagen, and (ii) accumulating advanced glycation end-products (AGEs) which form protein-protein cross-links along the collagen molecules (Hayashi and Hirayama, 2017; Wagenseil and Mecham, 2012) – for a review on collagen glycation as a potential driver of connective tissue disease see Snedeker and Gautieri (2014). For background on the chemistry of cross-linking of collagen and elastin we refer to the study of Eyre et al. (1984).

The effect of the mechanical properties of AGEs was also investigated by Svensson et al. (2018) for tendons. Inhibition of the formation of AGE-induced cross-links reduces the stiffness of large arteries in rats; see Greenwald (2007) and references therein. The study of Uzel and Buehler (2011) developed a simple molecular model of the cross-link structure of type I collagen and showed that the presence of the cross-links resulted in strengthening of the collagen structure at large deformations. The study of Yang et al. (2012) investigated the influence of different cross-links on the stress relaxation behavior of collagen fibrils. Experimental data were analyzed using a two-term Prony series, which suggested that fast relaxation is related to the relative sliding of collagen microfibrils and that the slow relaxation process resulted from the collagen molecules for which there is a larger number of cross-links. The paper of Davidenko et al. (2015) examined how different levels of cross-linking of collagenous-based scaffolds effect their mechanical properties. The study of Kwansa et al. (2016) used molecular-dynamics simulations based on collagen type I microfibril units of both uncross-linked and cross-linked fibrils. In particular, in Kwansa et al. (2016) uniaxial tension tests were simulated to examine the effect of the cross-linking on the elastic moduli, thus showing that the different cross-link types led to no alterations in the low-strain moduli while the finite strain elastic modulus was significantly increased.

One continuum-based 3D model taking account of cross-linking was proposed by Sáez et al. (2014). The cross-links were accounted for by a parameter which provided a weighting between the isotropic and the anisotropic response. The model was used to fit data from uniaxial tests on pig carotid arteries for which the cross-linking was unknown, in which case the relevance of a model accounting for cross-linking is unclear. Another 3D continuum arterial constitutive model considering collagen content and cross-linking was proposed by Tian et al. (2016). That approach is based on the eight-chain model, which was developed to characterize rubber-like materials but is unsuitable for fibrous tissues. Based on a discrete network of cross-linked biopolymer fibers (Žagar et al., 2015) uses a computational approach to determine the stiffening effects of the cross-links, while in Lin and Gu (2015) a similar computational model was used to determine the effect of cross-link density and stiffness in a collagen gel. On the other hand, on the basis of Buehler (2006), Buehler (2008) proposed a 1D nanoscale model which considers the effect of different cross-link densities on the mechanical response of collagen fibrils. More details of the effect of the cross-link structure on the mechanical properties of collagen fibrils have been considered by Depalle et al. (2015) with particular reference to enzymatic cross-links. The review article of Eekhoff et al. (2018) describes the mechanical effects of collagen cross-linking specifically for tendons, while the paper of Yoshida et al. (2014) documents the mechanical properties of mouse cervical tissue with respect to collagen cross-links. The study of Chen et al. (2017) considers a collagen network for articular cartilage based on a spring-node model of cross-linked collagen, and the authors studied changes of the cross-link stiffness and density on the mechanical response.

The number of cross-links has a significant effect on the measures of the elastic modulus. This suggests that material parameters in a constitutive model should be dependent on the proportion and arrangement of cross-links within the collagen structure. Two key ingredients are the collagen fiber content, as measured by, e.g., the volume fractions of collagen and cross-links, and the relative arrangement.

The purpose of this paper is to characterize the effect of cross-links on the basis of a phenomenological continuum model that takes account of information about cross-links at the micro-structure level. Although there are some approaches documented in the literature, as mentioned above, there is not yet a fully 3D model available that describes, e.g., the anisotropic response of arterial walls that takes proper account of collagen cross-linking.

In the present study we first consider a continuum approach that involves the cross-link density and a cross-link-dependent stiffness, which is a rather simple phenomenological approach. For this model we specialize to uniaxial extension and examine the effects of varying cross-link densities on the mechanical response of the material. Second, we consider explicitly the relative orientation of the collagen fibers and the cross-links and their interactions using an invariant-based energy function that incorporates contributions from the matrix material, collagen fibers, the cross-links and their interactions with the fibers. For the second approach we also illustrate uniaxial extension and analyze the influence of different cross-link arrangements and material parameters. Finally, we consider a model with two families of fibers arranged in 3D, with the fibers aligned within each family, and with two sets of aligned cross-links connecting the fibers in each family. This general formulation is suitable for finite element implementation, and towards this aim we provide the elasticity tensor associated with the model in an appendix.

We also consider a planar specialization of the model and illustrate it by application to a simple shear deformation, showing the effect of the cross-link orientation (relative to the fibers) and cross-link density on the shear stress versus amount of shear deformation. The reader who requires additional information on the subject of nonlinear elasticity and solid mechanics is referred to the monographs of Holzapfel (2000) and Ogden (1997), while a detailed explanation of the underlying constitutive theory for strongly anisotropic solids can be found in Spencer (1984).

2. Model structure

Suppose the collagen fibers are embedded within an isotropic matrix with the volume fraction Φ so that $(1 - \Phi)$ is the volume fraction of the matrix. Let the elastic properties of the matrix and fibers be described in terms of strain-energy functions Ψ_{iso} and Ψ_f , respectively. We consider Ψ_{iso} to depend on the isotropic invariant $I_1 = \text{tr } \mathbf{C}$, where $\mathbf{C} = \mathbf{F}^T \mathbf{F}$ is the right Cauchy–Green tensor, \mathbf{F} is the deformation gradient, and Ψ_f , the energy associated with the fiber in the direction \mathbf{M} in the reference configuration, to depend on $I_4 = \mathbf{M} \cdot \mathbf{C} \mathbf{M}$ and also on a measure of the density of cross-links per unit length of the fiber in the direction \mathbf{M} .

We consider the material to be incompressible ($J \equiv \det \mathbf{F} = 1$) with the total elastic energy of this composite as

$$\Psi(I_1, I_4, \rho) = (1 - \Phi)\Psi_{\text{iso}}(I_1) + \Phi\Psi_f(I_4, \rho), \quad (1)$$

where ρ can be thought of as the number of cross-links per unit length, subsequently referred to as the density of cross-links with dimension $1/(\text{length})$. As an example Ψ_{iso} can take on a neo-Hookean form, while for Ψ_f we could have $k(\rho)(I_4 - 1)^2/2$, a standard reinforcing model. Herein $k(\rho)$ is the cross-link-dependent fiber stiffness. Note that the derivative k' should be positive to reflect the increasing stiffness with increasing density of cross-links. Hence, from (1), the Cauchy stress tensor $\boldsymbol{\sigma}$ can be calculated as

$$\boldsymbol{\sigma} = \mathbf{F} \frac{\partial \Psi}{\partial \mathbf{F}} - p \mathbf{I} = (1 - \Phi)\mu \mathbf{b} + 2\Phi k(\rho)(I_4 - 1)\mathbf{m} \otimes \mathbf{m} - p \mathbf{I}, \quad (2)$$

where p is the Lagrange multiplier associated with the incompressibility constraint, \mathbf{b} denotes the left Cauchy–Green tensor, \mathbf{I} is the identity tensor, μ is the shear modulus of the neo-Hookean matrix and $\mathbf{m} = \mathbf{F} \mathbf{M}$. The anisotropic term is only active if $I_4 > 1$, so under compression in the fiber direction, the matrix bears the stress.

Because of the experimental data of fibrous tissue it is useful to represent Ψ_f as an exponential, in this case given by

$$\Psi_f = \frac{k_1(\rho)}{2k_2} \{\exp[k_2(I_4 - 1)^2] - 1\}, \quad (3)$$

where $k_1 > 0$ is a parameter with the dimension of stress, while $k_2 > 0$ is a dimensionless parameter. The Cauchy stress of the fibers is then denoted by $\boldsymbol{\sigma}_f$, i.e.

$$\boldsymbol{\sigma}_f = 2\Phi k_1(\rho)(I_4 - 1) \exp[k_2(I_4 - 1)^2] \mathbf{m} \otimes \mathbf{m}, \quad (4)$$

while the Cauchy stress for the matrix $\boldsymbol{\sigma}_{\text{iso}}$ is

$$\boldsymbol{\sigma}_{\text{iso}} = (1 - \Phi)\mu \mathbf{b}. \quad (5)$$

Let us now consider a strip of tissue in the axial/circumferential plane with two families of fibers which are arranged symmetrically with respect to the axes, as indicated in Fig. 1, where α is the angle between the axial direction and the direction of each family of fibers. The direction of the second fiber family is denoted by \mathbf{M}' with $\mathbf{m}' = \mathbf{F} \mathbf{M}'$. According to Fig. 1 the matrix forms of \mathbf{M} and \mathbf{M}' are

$$[\mathbf{M}] = [\cos \alpha, \sin \alpha, 0]^T, \quad [\mathbf{M}'] = [\cos \alpha, -\sin \alpha, 0]^T, \quad (6)$$

where we have assumed that the collagen fibers have no out-of-plane component. A push forward gives

$$[\mathbf{m}] = [\lambda_1 \cos \alpha, \lambda_2 \sin \alpha, 0]^T, \quad [\mathbf{m}'] = [\lambda_1 \cos \alpha, -\lambda_2 \sin \alpha, 0]^T, \quad (7)$$

where λ_1 and λ_2 are the principal stretches along the directions 1 (axial direction) and 2 (circumferential direction), respectively, while, from the incompressibility condition, $\lambda_3 = \lambda_1^{-1} \lambda_2^{-1}$. The invariant I_4 is then

$$I_4 = \mathbf{M} \cdot \mathbf{C} \mathbf{M} = \lambda_1^2 \cos^2 \alpha + \lambda_2^2 \sin^2 \alpha, \quad (8)$$

and by symmetry we have $\mathbf{M}' \cdot \mathbf{C} \mathbf{M}' = I_4$.

The Cauchy stress tensor $\boldsymbol{\sigma} = \boldsymbol{\sigma}_{\text{iso}} + \boldsymbol{\sigma}_f - p \mathbf{I}$ then becomes

$$\boldsymbol{\sigma} = (1 - \Phi)\mu \mathbf{b} + 2\Phi k_1(\rho)(I_4 - 1) \exp[k_2(I_4 - 1)^2] (\mathbf{m} \otimes \mathbf{m} + \mathbf{m}' \otimes \mathbf{m}') - p \mathbf{I}, \quad (9)$$

which is diagonal with respect to the chosen axes (no shear stress), and hence its components are

$$\sigma_{11} = (1 - \Phi)\mu \lambda_1^2 + 4\Phi k_1(\rho)(I_4 - 1) \exp[k_2(I_4 - 1)^2] \lambda_1^2 \cos^2 \alpha - p, \quad (10)$$

$$\sigma_{22} = (1 - \Phi)\mu \lambda_2^2 + 4\Phi k_1(\rho)(I_4 - 1) \exp[k_2(I_4 - 1)^2] \lambda_2^2 \sin^2 \alpha - p, \quad (11)$$

$$\sigma_{33} = (1 - \Phi)\mu \lambda_3^2 - p. \quad (12)$$

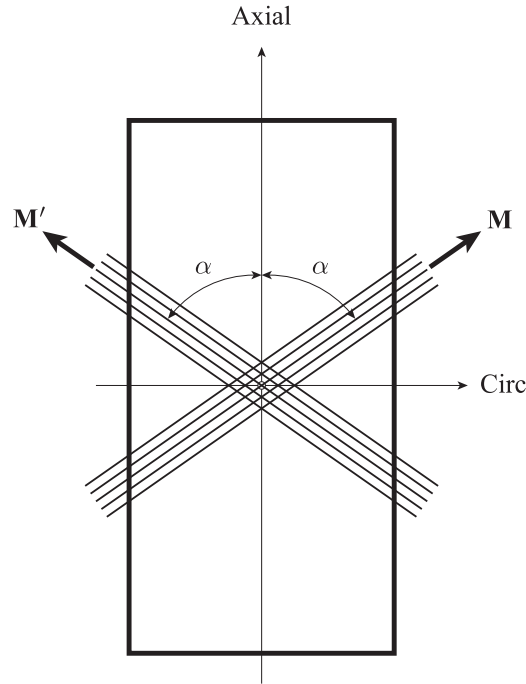


Fig. 1. Sketch of a rectangular tissue strip reinforced by two in-plane families of aligned fibers symmetric with respect to its edges, with fiber angle α .

We assume that the strip is under plane stress conditions with loads parallel to the circumferential and axial directions. Then the stress σ_{33} is zero which allows for p to be eliminated from (10) and (11) to give

$$\sigma_{11} = (1 - \Phi)\mu(\lambda_1^2 - \lambda_3^2) + 4\Phi k_1(\rho)(I_4 - 1) \exp[k_2(I_4 - 1)^2] \lambda_1^2 \cos^2 \alpha, \quad (13)$$

$$\sigma_{22} = (1 - \Phi)\mu(\lambda_2^2 - \lambda_3^2) + 4\Phi k_1(\rho)(I_4 - 1) \exp[k_2(I_4 - 1)^2] \lambda_2^2 \sin^2 \alpha, \quad (14)$$

where I_4 is given by (8)₂, and λ_3 by the incompressibility condition. Thus, σ_{11} and σ_{22} are given in terms of λ_1 and λ_2 . By considering uniaxial stress with $\sigma_{22} = 0$, Eq. (14) can in principle be solved for λ_2 as a function of λ_1 , and then σ_{11} is a function of λ_1 alone.

We now focus on a special case, namely $\alpha = 0$. Hence, the two families of fibers coincide and the direction of the collagen fibers is the axial direction. For this case we choose $\lambda = \lambda_1$, so by symmetry $\lambda_2 = \lambda_3 = \lambda^{-1/2}$, and according to (8)₂ we have $I_4 = \lambda^2$. We use the dimensionless quantities $\bar{\sigma}_{11} = \sigma_{11}/\mu$ and $\bar{k}_1 = k_1/\mu$, and obtain

$$\bar{\sigma}_{11} = (1 - \Phi)(\lambda^2 - \lambda^{-1}) + 4\Phi \bar{k}_1(\rho)(\lambda^2 - 1)\lambda^2 \exp[k_2(\lambda^2 - 1)^2] \quad (15)$$

from (13), which is an explicit expression for $\bar{\sigma}_{11}$ in terms of λ , where Φ , $\bar{k}_1(\rho)$ and k_2 need to be specified.

The functional dependence of \bar{k}_1 on ρ can be modeled by any suitable function but for simplicity of illustration we consider the quadratic equation $\bar{k}_1 = \bar{k}_0 + \bar{a}\rho^2$, where $\bar{k}_0 \geq 0$ is the value of \bar{k}_1 at $\rho = 0$ and $\bar{a} > 0$ is a parameter with dimension (length)².

Fig. 2 illustrates the influence of the density of cross-links on the uniaxial response in the direction of the fibers. For particular values of the parameters we have used $\Phi = 0.1$, $\bar{k}_0 = 0.1$, $\bar{a} = 0.25$ and $k_2 = 0.3$. The four curves in the figure correspond to the four values of ρ , i.e. 0, 1, 2, and 3. Note in particular the case $\rho = 0$ for which there are no cross-links and the tension is supported by the fibers and the matrix without cross-links, as reflected in the lower value of the tension. As ρ increases the response becomes stiffer.

3. A model with aligned collagen fibers connected by separately aligned cross-links

We consider collagen fibers to be in the direction of the unit vector \mathbf{E}_1 and let \mathbf{E}_R be the radial unit vector normal to that direction. In addition we consider two symmetrically disposed families of cross-links in the directions of the unit vectors \mathbf{L}^+ and \mathbf{L}^- (\mathbf{L} stands for link), which are defined by

$$\mathbf{L}^\pm = \pm \cos \alpha_0 \mathbf{E}_1 + \sin \alpha_0 \mathbf{E}_R, \quad (16)$$

where α_0 defines their orientation relative to the collagen fiber direction; see Fig. 3.

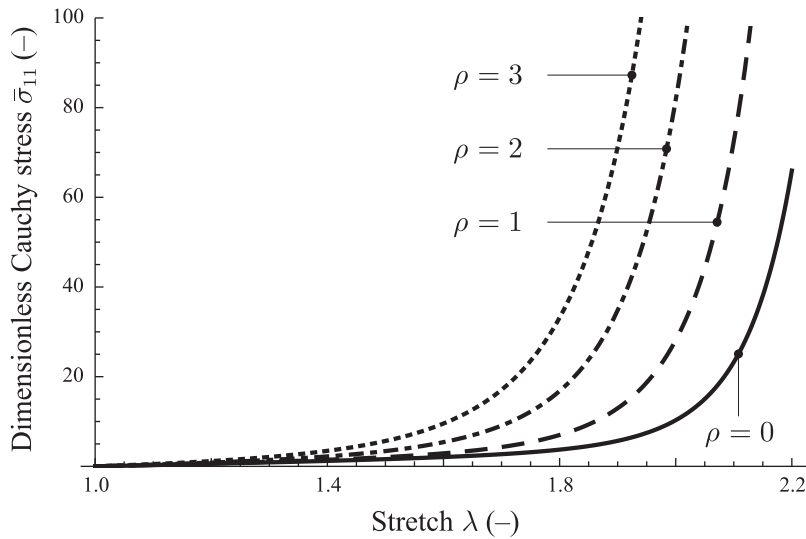


Fig. 2. Plots of the dimensionless Cauchy stress $\bar{\sigma}_{11}$ versus the stretch λ for four different values of density of cross-links ρ , including $\rho = 0$ (no cross-links).

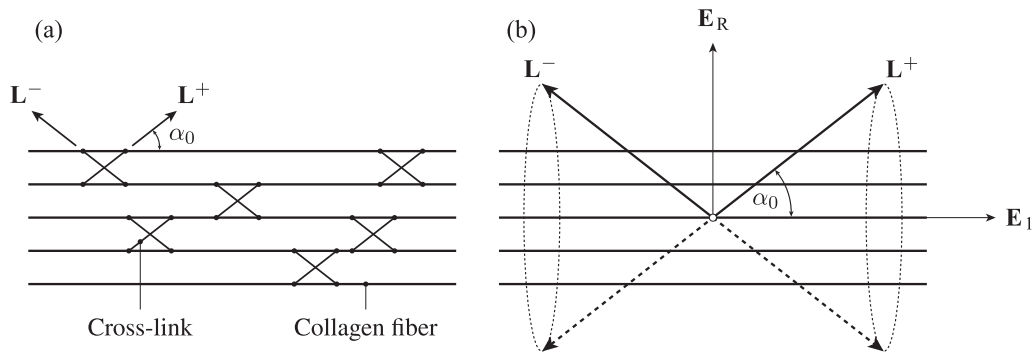


Fig. 3. (a) Aligned collagen fibers in the direction \mathbf{E}_1 with two families of aligned interconnecting cross-links with directions \mathbf{L}^+ and \mathbf{L}^- making an angle α_0 with \mathbf{E}_1 . (b) Focus on a pair of cross-links in (a), indicating their rotational symmetry about \mathbf{E}_1 with the radial vector \mathbf{E}_R .

A uniaxial deformation with stretch λ is applied along the collagen fibers so that by symmetry and considering the material to be incompressible the deformation gradient has the form

$$\mathbf{F} = \lambda \mathbf{E}_1 \otimes \mathbf{E}_1 + \lambda^{-1/2} \mathbf{E}_R \otimes \mathbf{E}_R. \tag{17}$$

We define $\mathbf{e} = \mathbf{F}\mathbf{E}_1 = \lambda \mathbf{E}_1$ and $\mathbf{e}_r = \mathbf{F}\mathbf{E}_R = \lambda^{-1/2} \mathbf{E}_R$ as the push-forwards of \mathbf{E}_1 and \mathbf{E}_R under the deformation. The corresponding push-forwards of \mathbf{L}^+ and \mathbf{L}^- are then

$$\mathbf{I}^\pm = \mathbf{F}\mathbf{L}^\pm = \pm \lambda \cos \alpha_0 \mathbf{E}_1 + \lambda^{-1/2} \sin \alpha_0 \mathbf{E}_R. \tag{18}$$

For this special deformation the isotropic invariant is given by $I_1 = \text{tr } \mathbf{C} = \lambda^2 + 2\lambda^{-1}$, while the squares of the stretches in the directions \mathbf{E}_1 , \mathbf{L}^+ and \mathbf{L}^- are

$$I_4 = \mathbf{e} \cdot \mathbf{e} = \mathbf{C}\mathbf{E}_1 \cdot \mathbf{E}_1 = \lambda^2, \quad I = \mathbf{I}^\pm \cdot \mathbf{I}^\pm = \lambda^2 \cos^2 \alpha_0 + \lambda^{-1} \sin^2 \alpha_0, \tag{19}$$

wherein the invariants I_4 and I are defined. For the cross-links to be extended, i.e. when $\lambda > 1$, α_0 has to be restricted according to

$$\cos^2 \alpha_0 > \frac{1}{\lambda^2 + \lambda + 1}, \tag{20}$$

which is satisfied for all $\lambda > 1$ if $\cos \alpha_0 > 1/\sqrt{3}$. The invariant I_4 is the square of the stretch in the collagen fibers and I is the square of the stretch in each of the cross-link directions. We also define the coupling between the collagen fiber and cross-link directions by the quantities I_8^+ and I_8^- , which are given by

$$I_8^\pm = \mathbf{I}^\pm \cdot \mathbf{e} = \pm \lambda^2 \cos \alpha_0. \tag{21}$$

These are not themselves invariants (their sign changes under reversal of either \mathbf{e} or \mathbf{I}^\pm), but $(I_8^+)^2 = (I_8^-)^2$ is invariant. The values of the invariants I_1 , I_4 , and I and the quantities I_8^\pm in the reference configuration are 3, 1, 1 and $\pm \cos \alpha_0$, respectively.

We now consider a strain-energy function Ψ , which is a function of I_1 , I_4 , I , I_8^+ and I_8^- . Specifically we consider Ψ to have the form

$$\Psi = (1 - \Phi - \Phi^*)\Psi_{\text{iso}}(I_1) + \Phi\Psi_f(I_4) + \Phi^*[\Psi_c(I) + \Psi_{\text{fc}}(I_8^+) + \Psi_{\text{fc}}(I_8^-)], \quad (22)$$

where Φ and Φ^* denote the volume fractions of the collagen fibers and the cross-links, respectively.

The functions Ψ_{iso} , Ψ_f and Ψ_c are the energies stored in the matrix material, the collagen fibers and the cross-links, respectively, while the two Ψ_{fc} -terms represent the interaction energies between the collagen fibers and the cross-links. Noting that $\Psi'_{\text{fc}}(I_8^-) = -\Psi'_{\text{fc}}(I_8^+)$, the Cauchy stress tensor σ can be written in the form

$$\sigma = -p\mathbf{I} + 2(1 - \Phi - \Phi^*)\Psi'_{\text{iso}}(I_1)\mathbf{b} + 2\Phi\Psi'_f(I_4)\mathbf{e} \otimes \mathbf{e} + \Phi^*\{2\Psi'_c(\mathbf{I}^+ \otimes \mathbf{I}^+ + \mathbf{I}^- \otimes \mathbf{I}^-) + \Psi'_{\text{fc}}(I_8^+)[\mathbf{e} \otimes \mathbf{I}^+ + \mathbf{I}^+ \otimes \mathbf{e} - (\mathbf{e} \otimes \mathbf{I}^- + \mathbf{I}^- \otimes \mathbf{e})]\}, \quad (23)$$

where we have used the abbreviations

$$\Psi'_{\text{iso}}(I_1) = \frac{\partial \Psi_{\text{iso}}}{\partial I_1}, \quad \Psi'_f(I_4) = \frac{\partial \Psi_f}{\partial I_4}, \quad \Psi'_c(I) = \frac{\partial \Psi_c}{\partial I}, \quad \Psi'_{\text{fc}}(I_8^\pm) = \frac{\partial \Psi_{\text{fc}}}{\partial I_8^\pm}. \quad (24)$$

Now, for the subsequent component forms we need

$$\mathbf{e} \otimes \mathbf{I}^+ + \mathbf{I}^+ \otimes \mathbf{e} - (\mathbf{e} \otimes \mathbf{I}^- + \mathbf{I}^- \otimes \mathbf{e}) = 4\lambda^2 \cos \alpha_0 \mathbf{E}_1 \otimes \mathbf{E}_1. \quad (25)$$

Hence, the stress components are

$$\sigma_{11} = -p + 2(1 - \Phi - \Phi^*)\Psi'_{\text{iso}}\lambda^2 + 2\Phi\Psi'_f\lambda^2 + 4\Phi^*\Psi'_c\lambda^2 \cos^2 \alpha_0 + 4\Phi^*\Psi'_{\text{fc}}\lambda^2 \cos \alpha_0, \quad (26)$$

$$0 = \sigma_{rr} = -p + 2(1 - \Phi - \Phi^*)\Psi'_{\text{iso}}\lambda^{-1} + 4\Phi^*\Psi'_c\lambda^{-1} \sin^2 \alpha_0, \quad (27)$$

where the argument of Ψ_{fc} is I_8^\pm . By eliminating the Lagrange multiplier p by subtraction of (27) from (26) we obtain the uniaxial stress $\sigma = \sigma_{11}$ as

$$\sigma = 2(1 - \Phi - \Phi^*)\Psi'_{\text{iso}}(\lambda^2 - \lambda^{-1}) + 2\Phi\Psi'_f\lambda^2 + 4\Phi^*\Psi'_c(\lambda^2 \cos^2 \alpha_0 - \lambda^{-1} \sin^2 \alpha_0) + 4\Phi^*\Psi'_{\text{fc}}\lambda^2 \cos \alpha_0. \quad (28)$$

Now let us consider some specific energy functions. For the matrix material we use the isotropic neo-Hookean material

$$\Psi_{\text{iso}} = \frac{1}{2}\mu(I_1 - 3), \quad (29)$$

where the constant μ is a positive parameter, and for the collagen fibers we use the standard exponential form, i.e.

$$\Psi_f = \frac{k_1}{2k_2} \{\exp[k_2(I_4 - 1)^2] - 1\}, \quad (30)$$

where $k_1 > 0$ is a stress-like constant and $k_2 > 0$ is a dimensionless constant.

There is very little if any information available about the mechanical properties of cross-links. Therefore, for simplicity of illustration, we make the assumption that Ψ_c has the quadratic reinforcing form

$$\Psi_c = \frac{1}{2}\nu(I - 1)^2, \quad (31)$$

where ν is a positive parameter with the dimension of stress that measures the strength of the cross-links, and is referred to as the cross-link parameter. Note that the constant k_1 in (30) is different from that in (3), and we now write it as k_0 temporarily. Then, by comparing the quadratic approximation of (3) with (30) and (31) we obtain $\nu + k_0 = k_1(\rho)$, which relates the cross-link stiffness ν to the cross-link density of the first model. Similarly to (31), for Ψ_{fc} we take the form

$$\Psi_{\text{fc}} = \frac{1}{2}\kappa(I_8^+ - \cos \alpha_0)^2 = \frac{1}{2}\kappa(I_8^- + \cos \alpha_0)^2, \quad (32)$$

where κ is also a positive stress-like parameter. It measures the strength of the interaction between the fibers and the cross-links. Hence, by using (24) and according to (28), the Cauchy stress σ has the form

$$\sigma = (1 - \Phi - \Phi^*)\mu(\lambda^2 - \lambda^{-1}) + 2\Phi k_1(\lambda^2 - 1)\lambda^2 \exp[k_2(\lambda^2 - 1)^2] + 4\Phi^*\nu(\lambda^2 \cos^2 \alpha_0 + \lambda^{-1} \sin^2 \alpha_0 - 1)(\lambda^2 \cos^2 \alpha_0 - \lambda^{-1} \sin^2 \alpha_0) + 4\Phi^*\kappa(\lambda^2 - 1)\lambda^2 \cos^2 \alpha_0. \quad (33)$$

In Fig. 4 we plot the dimensionless stress $\bar{\sigma} = \sigma/\mu$ against the stretch λ for a representative selection of the parameters involved in (33). Fig. 4(a) shows how the response depends on the orientation α_0 of the cross-links for a fixed value of $\bar{\nu} = \nu/\mu$, while Fig. 4(b) illustrates the dependence on $\bar{\nu}$ for a fixed value of α_0 , in each case for fixed values of the other parameters, as specified in the caption of Fig. 4. It is clear that the cross-links stiffen the response. In Fig. 4(a) the response becomes stiffer as the cross-links become more aligned with the fibers, much stiffer than in the absence of cross-links, while Fig. 4(b) shows that an increase in the density of the cross-links likewise stiffens the response.

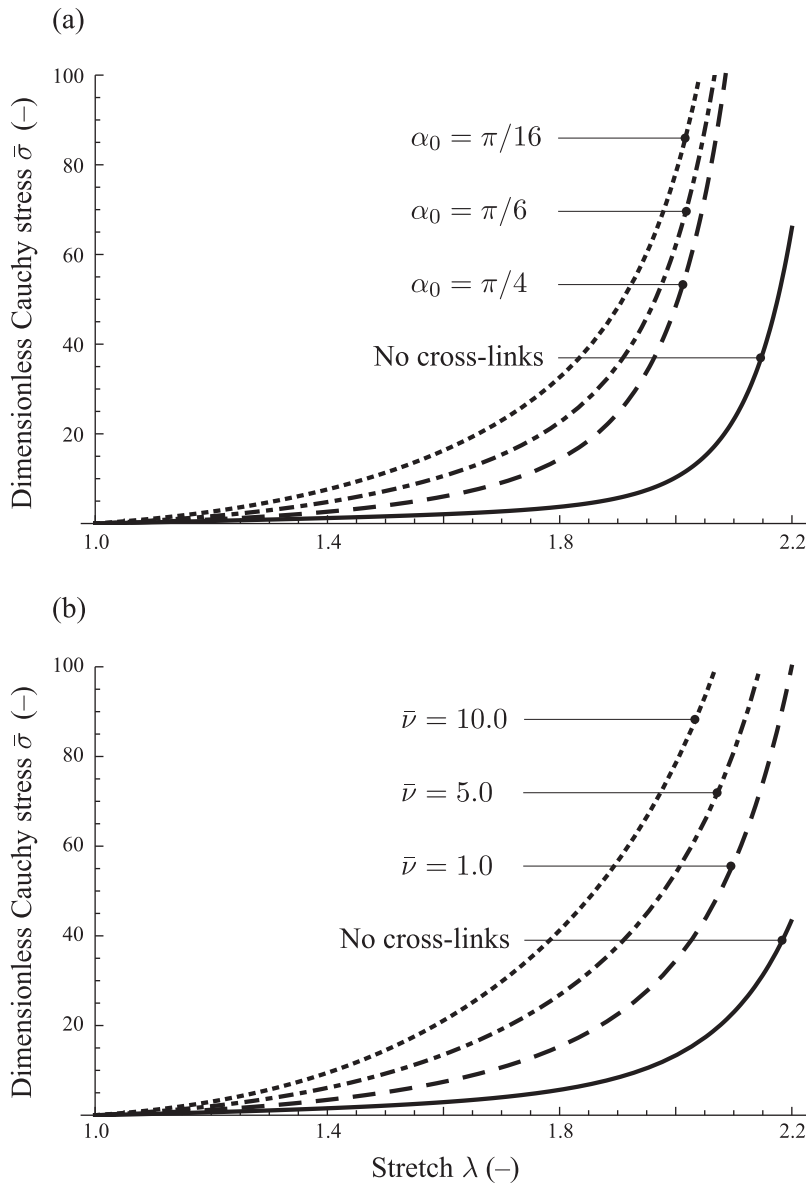


Fig. 4. Plots of the dimensionless Cauchy stress $\bar{\sigma} = \sigma/\mu$ versus the stretch λ : (a) for three values of the cross-link angle α_0 ($\pi/16$, $\pi/6$, $\pi/4$) compared with the plot for the case of no cross-links. On the basis of (33) the following parameters were used $\Phi = 0.1$, $\Phi^* = 0.15$, $k_1 = k_1/\mu = 1$, $k_2 = 0.3$, $\bar{\nu} = \nu/\mu = 5$, $\bar{\kappa} = \kappa/\mu = 1$; (b) for four values of the dimensionless cross-link parameter $\bar{\nu}$ (10.0, 5.0, 1.0, 0). On the basis of (33) the following parameters were used $\Phi = 0.2$, $\Phi^* = 0.2$, $k_1 = 1$, $k_2 = 0.16$, $\alpha_0 = \pi/6$, $\bar{\kappa} = 1$.

4. Formulation for a general fiber direction

In the previous section we considered a special deformation with the fiber directions aligned with the axis \mathbf{E}_1 of extension. In the present section we generalize this for an arbitrary fiber direction and the corresponding cross-links. Consider the axis \mathbf{E}_1 and the associated rectangular Cartesian axes \mathbf{E}_2 and \mathbf{E}_3 , which are depicted in Fig. 5. To arrange the initial general geometry we rotate the system by means of the rotation tensor \mathbf{Q} such that the unit basis vectors \mathbf{e}_i , $i = 1, 2, 3$, become

$$\mathbf{e}_i = \mathbf{Q}\mathbf{E}_i, \quad i = 1, 2, 3, \tag{34}$$

where

$$\mathbf{Q} = \mathbf{e}_1 \otimes \mathbf{E}_1 + \mathbf{e}_2 \otimes \mathbf{E}_2 + \mathbf{e}_3 \otimes \mathbf{E}_3, \tag{35}$$

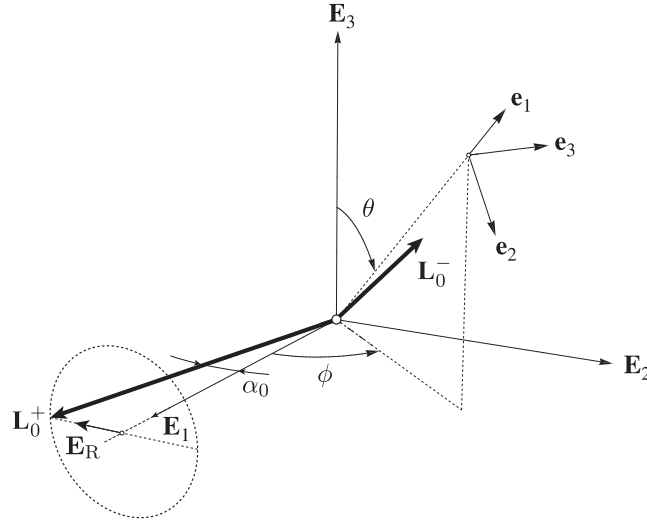


Fig. 5. Rectangular Cartesian axes $\mathbf{E}_1, \mathbf{E}_2, \mathbf{E}_3$ transformed into orthonormal axes $\mathbf{e}_1, \mathbf{e}_2, \mathbf{e}_3$, where the transformation is a function of the two spherical polar angles θ and ϕ . \mathbf{E}_1 represents the fiber direction and, according to (39), \mathbf{L}_0^\pm are the directions of representative cross-links, which are rotationally symmetric with respect to $\pm \mathbf{E}_1$. \mathbf{E}_R represents an arbitrary unit vector normal to \mathbf{E}_1 .

and hence with respect to spherical polar coordinates θ and ϕ shown in Fig. 5

$$\mathbf{e}_1 = \sin \theta \cos \phi \mathbf{E}_1 + \sin \theta \sin \phi \mathbf{E}_2 + \cos \theta \mathbf{E}_3, \tag{36}$$

$$\mathbf{e}_2 = \cos \theta \cos \phi \mathbf{E}_1 + \cos \theta \sin \phi \mathbf{E}_2 - \sin \theta \mathbf{E}_3, \tag{37}$$

$$\mathbf{e}_3 = -\sin \phi \mathbf{E}_1 + \cos \phi \mathbf{E}_2, \tag{38}$$

with \mathbf{e}_1 now identified as the collagen fiber direction.

Here the directions of two symmetrically disposed families of cross-links are denoted by the unit vectors \mathbf{L}_0^+ and \mathbf{L}_0^- , as distinct from the notation \mathbf{L}^\pm used in (16), so that

$$\mathbf{L}_0^\pm = \pm \cos \alpha_0 \mathbf{E}_1 + \sin \alpha_0 \mathbf{E}_R, \tag{39}$$

where \mathbf{E}_R , which is an arbitrary vector orthogonal to \mathbf{E}_1 , can be written as

$$\mathbf{E}_R = \cos \phi_0 \mathbf{E}_2 + \sin \phi_0 \mathbf{E}_3, \tag{40}$$

with ϕ_0 arbitrary. Then we define \mathbf{L}^\pm according to

$$\mathbf{L}^\pm = \mathbf{Q} \mathbf{L}_0^\pm = \pm \cos \alpha_0 \mathbf{e}_1 + \sin \alpha_0 \mathbf{e}_r, \quad \mathbf{e}_r = \mathbf{Q} \mathbf{E}_R = \cos \phi_0 \mathbf{e}_2 + \sin \phi_0 \mathbf{e}_3. \tag{41}$$

Now on application of a deformation gradient \mathbf{F} the invariant I_4 associated with the fiber direction is given by

$$I_4 = (\mathbf{F} \mathbf{e}_1) \cdot (\mathbf{F} \mathbf{e}_1) = (\mathbf{C} \mathbf{e}_1) \cdot \mathbf{e}_1. \tag{42}$$

It follows from (41)₁ that

$$\mathbf{F} \mathbf{L}^\pm = \pm \cos \alpha_0 \mathbf{F} \mathbf{e}_1 + \sin \alpha_0 \mathbf{F} \mathbf{e}_r. \tag{43}$$

Hence, the invariants I^\pm , and the quantities I_8^\pm describing the coupling between the collagen fiber and cross-link directions are

$$I^\pm = (\mathbf{F} \mathbf{L}^\pm) \cdot (\mathbf{F} \mathbf{L}^\pm) = c_0^2 I_4 \pm 2s_0 c_0 (\mathbf{C} \mathbf{e}_1) \cdot \mathbf{e}_r + s_0^2 (\mathbf{C} \mathbf{e}_r) \cdot \mathbf{e}_r, \tag{44}$$

$$I_8^\pm = (\mathbf{F} \mathbf{e}_1) \cdot (\mathbf{F} \mathbf{L}^\pm) = \pm c_0 I_4 + s_0 (\mathbf{C} \mathbf{e}_1) \cdot \mathbf{e}_r, \tag{45}$$

where for conciseness we have written $s_0 = \sin \alpha_0$ and $c_0 = \cos \alpha_0$. Note that, in general, $I^+ \neq I^-$ and $I_8^+ \neq -I_8^-$, which is unlike the case of the uniaxial tension considered in Section 3.

Next we note the derivatives of the invariants I_4, I^\pm and the quantities I_8^\pm with respect to the right Cauchy–Green tensor \mathbf{C} , i.e.

$$\frac{\partial I_4}{\partial \mathbf{C}} = \mathbf{e}_1 \otimes \mathbf{e}_1, \tag{46}$$

$$\frac{\partial I^\pm}{\partial \mathbf{C}} = c_0^2 \mathbf{e}_1 \otimes \mathbf{e}_1 \pm s_0 c_0 (\mathbf{e}_1 \otimes \mathbf{e}_r + \mathbf{e}_r \otimes \mathbf{e}_1) + s_0^2 \mathbf{e}_r \otimes \mathbf{e}_r, \quad (47)$$

$$\frac{\partial I_8^\pm}{\partial \mathbf{C}} = \pm c_0 \mathbf{e}_1 \otimes \mathbf{e}_1 + \frac{1}{2} s_0 (\mathbf{e}_1 \otimes \mathbf{e}_r + \mathbf{e}_r \otimes \mathbf{e}_1). \quad (48)$$

Now let us consider the strain-energy function $\Psi(I_1, I_4, I^+, I^-, I_8^+, I_8^-)$ so that

$$\begin{aligned} \boldsymbol{\sigma} = & -p\mathbf{I} + 2\psi_1 \mathbf{b} + 2\psi_4 \mathbf{Fe}_1 \otimes \mathbf{Fe}_1 + 2\psi_{I^+} [c_0^2 \mathbf{Fe}_1 \otimes \mathbf{Fe}_1 + s_0 c_0 (\mathbf{Fe}_1 \otimes \mathbf{Fe}_r + \mathbf{Fe}_r \otimes \mathbf{Fe}_1) + s_0^2 \mathbf{Fe}_r \otimes \mathbf{Fe}_r] \\ & + 2\psi_{I^-} [c_0^2 \mathbf{Fe}_1 \otimes \mathbf{Fe}_1 - s_0 c_0 (\mathbf{Fe}_1 \otimes \mathbf{Fe}_r + \mathbf{Fe}_r \otimes \mathbf{Fe}_1) + s_0^2 \mathbf{Fe}_r \otimes \mathbf{Fe}_r] \\ & + \psi_{8^+} [2c_0 \mathbf{Fe}_1 \otimes \mathbf{Fe}_1 + s_0 (\mathbf{Fe}_1 \otimes \mathbf{Fe}_r + \mathbf{Fe}_r \otimes \mathbf{Fe}_1)] + \psi_{8^-} [-2c_0 \mathbf{Fe}_1 \otimes \mathbf{Fe}_1 + s_0 (\mathbf{Fe}_1 \otimes \mathbf{Fe}_r + \mathbf{Fe}_r \otimes \mathbf{Fe}_1)], \end{aligned} \quad (49)$$

where we have used the abbreviations $\psi_1 = \partial\Psi/\partial I_1$, $\psi_4 = \partial\Psi/\partial I_4$, $\psi_{I^\pm} = \partial\Psi/\partial I^\pm$ and $\psi_{8^\pm} = \partial\Psi/\partial I_8^\pm$. This is the most general Cauchy stress expression for parallel collagen fibers with cross-links of the type indicated. For the related elasticity tensor in the material description see the Appendix.

To recover the uniaxial case (Section 3) from the general equations in this section we have $\mathbf{e}_1 = \mathbf{E}_1$ for uniaxial tension, and consequently

$$\mathbf{Fe}_1 = \lambda \mathbf{e}_1, \quad \mathbf{Fe}_r = \lambda^{-1/2} \mathbf{e}_r, \quad \mathbf{FL}^\pm = \pm c_0 \lambda \mathbf{e}_1 + s_0 \lambda^{-1/2} \mathbf{e}_r. \quad (50)$$

Then, with $I_4 = \lambda^2$ we obtain from (44) and (45)

$$I \equiv I^\pm = c_0^2 \lambda^2 + s_0^2 \lambda^{-1}, \quad I_8 = I_8^+ = c_0 \lambda^2, \quad I_8^- = -I_8^+. \quad (51)$$

Then

$$\psi_{I^+} = \psi_{I^-} = \psi_{I^-}, \quad \psi_{8^+} = -\psi_{8^-} = \psi_{8^-}, \quad (52)$$

and (49) specializes to

$$\boldsymbol{\sigma} = -p\mathbf{I} + 2\psi_1 (\lambda^2 \mathbf{e}_1 \otimes \mathbf{e}_1 + \lambda^{-1} \mathbf{e}_r \otimes \mathbf{e}_r) + 2\psi_4 \lambda^2 \mathbf{e}_1 \otimes \mathbf{e}_1 + 4\psi_{I^+} (c_0^2 \lambda^2 \mathbf{e}_1 \otimes \mathbf{e}_1 + s_0^2 \lambda^{-1} \mathbf{e}_r \otimes \mathbf{e}_r) + 4\psi_{8^+} c_0 \lambda^2 \mathbf{e}_1 \otimes \mathbf{e}_1. \quad (53)$$

The related components are

$$\sigma = \sigma_{11} = -p + 2\psi_1 \lambda^2 + 2\psi_4 \lambda^2 + 4\psi_{I^+} c_0^2 \lambda^2 + 4\psi_{8^+} c_0 \lambda^2, \quad (54)$$

$$0 = \sigma_{rr} = -p + 2\psi_1 \lambda^{-1} + 4\psi_{I^+} s_0^2 \lambda^{-1}. \quad (55)$$

By eliminating the Lagrange multiplier p we obtain

$$\sigma = 2\psi_1 (\lambda^2 - \lambda^{-1}) + 2\psi_4 \lambda^2 + 4\psi_{I^+} (c_0^2 \lambda^2 - s_0^2 \lambda^{-1}) + 4\psi_{8^+} c_0 \lambda^2. \quad (56)$$

Now let us use the specific strain-energy functions (29)–(32), i.e.

$$\Psi = \frac{1}{2} \mu (I_1 - 3) + \frac{k_1}{2k_2} \{ \exp[k_2 (I_4 - 1)^2] - 1 \} + \frac{1}{2} \nu (I - 1)^2 + \frac{1}{2} \kappa (I_8 - c_0)^2, \quad (57)$$

which gives with (56) the same expression for σ as in (33) except that here the volume fractions are incorporated into the material constants μ , k_1 , ν and κ .

4.1. Planar formulation

Next we consider the situation in which the fibers and cross-links are restricted to the $(\mathbf{E}_1, \mathbf{E}_2)$ plane and we define the fiber direction \mathbf{e}_1 and its normal \mathbf{e}_r as

$$\mathbf{e}_1 = \cos \alpha \mathbf{E}_1 + \sin \alpha \mathbf{E}_2, \quad \mathbf{e}_r = -\sin \alpha \mathbf{E}_1 + \cos \alpha \mathbf{E}_2, \quad (58)$$

where α is the angle between the fiber direction and the \mathbf{E}_1 axis (see Fig. 6).

With respect to \mathbf{e}_1 and \mathbf{e}_r the cross-link directions \mathbf{L}^\pm are defined by

$$\mathbf{L}^\pm = \pm c_0 \mathbf{e}_1 + s_0 \mathbf{e}_r, \quad (59)$$

which has the same form as (41)₁. The invariant $I_4 = (\mathbf{Ce}_1) \cdot \mathbf{e}_1$, as in (42)₂, but with \mathbf{e}_1 now defined by (58). We also have

$$\mathbf{FL}^\pm = \pm c_0 \mathbf{Fe}_1 + s_0 \mathbf{Fe}_r, \quad (60)$$

which is the same expression as (43) and the invariants I^\pm and the quantities I_8^\pm are again given by (44) and (45). The Cauchy stress tensor $\boldsymbol{\sigma}$ has the same form (49) as in 3D but now restricted to 2D.

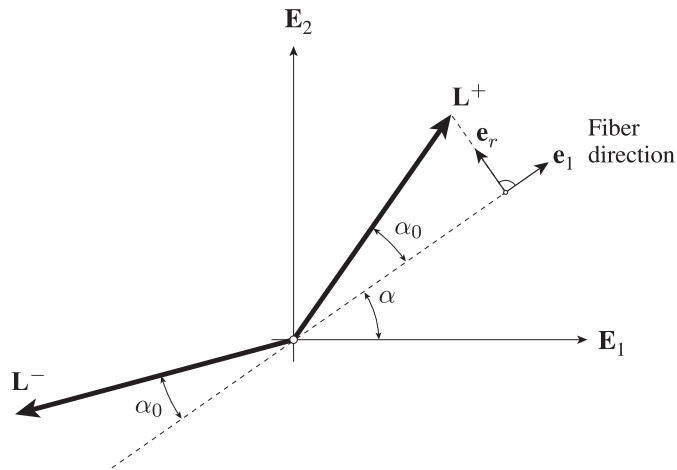


Fig. 6. Illustration showing a planar version of Fig. 5. In particular, \mathbf{e}_1 represents the fiber direction with unit normal \mathbf{e}_r , with respect to background axes \mathbf{E}_1 and \mathbf{E}_2 , while \mathbf{e}_1 makes an angle α with respect to the \mathbf{E}_1 -direction. \mathbf{L}^\pm represent the directions of two families of cross-links, and \mathbf{L}^\pm make an angle α_0 with respect to the $\pm \mathbf{e}_1$ direction.

4.1.1. Simple shear case

For simple shear in the \mathbf{E}_1 direction in the considered plane, the deformation gradient is given by $\mathbf{F} = \mathbf{I} + \gamma \mathbf{E}_1 \otimes \mathbf{E}_2$, where γ is the amount of shear. It follows that

$$\mathbf{F}\mathbf{e}_1 = \mathbf{e}_1 + \gamma \sin \alpha \mathbf{E}_1, \quad \mathbf{F}\mathbf{e}_r = \mathbf{e}_r + \gamma \cos \alpha \mathbf{E}_1. \tag{61}$$

The invariant $I_4 = (\mathbf{C}\mathbf{e}_1) \cdot \mathbf{E}_1$ is

$$I_4 = 1 + \gamma \sin 2\alpha + \gamma^2 \sin^2 \alpha, \tag{62}$$

while the required expressions $(\mathbf{C}\mathbf{e}_r) \cdot \mathbf{e}_r$ and $(\mathbf{C}\mathbf{e}_1) \cdot \mathbf{e}_r$ are given by

$$(\mathbf{C}\mathbf{e}_r) \cdot \mathbf{e}_r = 1 - \gamma \sin 2\alpha + \gamma^2 \cos^2 \alpha, \quad (\mathbf{C}\mathbf{e}_1) \cdot \mathbf{e}_r = \gamma \cos 2\alpha + \gamma^2 \sin \alpha \cos \alpha. \tag{63}$$

On substitution of (63) into (44)₂ and (45)₂ we obtain

$$I^\pm = 1 + \gamma \sin 2(\alpha \pm \alpha_0) + \gamma^2 \sin^2(\alpha \pm \alpha_0), \tag{64}$$

$$I_8^\pm = \pm c_0 + \gamma \sin(\alpha_0 \pm 2\alpha) + \gamma^2 \sin \alpha \sin(\alpha_0 \pm \alpha). \tag{65}$$

From (49) the components of the Cauchy stress are then given by

$$\begin{aligned} \sigma_{11} = & -p + 2\psi_1(1 + \gamma^2) + 2[\psi_4 + c_0^2(\psi_{I^+} + \psi_{I^-}) + c_0(\psi_{8^+} - \psi_{8^-})](c + \gamma s)^2 \\ & + 2s_0[2c_0(\psi_{I^+} - \psi_{I^-}) + \psi_{8^+} + \psi_{8^-}][(\gamma^2 - 1)sc + \gamma(c^2 - s^2)] + 2s_0^2(\psi_{I^+} + \psi_{I^-})(\gamma c - s)^2, \end{aligned} \tag{66}$$

$$\begin{aligned} \sigma_{22} = & -p + 2\psi_1 + 2[\psi_4 + c_0^2(\psi_{I^+} + \psi_{I^-}) + c_0(\psi_{8^+} - \psi_{8^-})]s^2 \\ & + 2s_0[2c_0(\psi_{I^+} - \psi_{I^-}) + \psi_{8^+} + \psi_{8^-}]sc + 2s_0^2(\psi_{I^+} + \psi_{I^-})c^2, \end{aligned} \tag{67}$$

$$\begin{aligned} \sigma_{12} = & 2\psi_1\gamma + 2[\psi_4 + c_0^2(\psi_{I^+} + \psi_{I^-}) + c_0(\psi_{8^+} - \psi_{8^-})]s(c + \gamma s) + s_0[2c_0(\psi_{I^+} - \psi_{I^-}) + \psi_{8^+} + \psi_{8^-}](c^2 - s^2 + 2\gamma sc) \\ & + 2s_0^2(\psi_{I^+} + \psi_{I^-})c(\gamma c - s) \equiv \frac{\partial \Psi}{\partial \gamma}, \end{aligned} \tag{68}$$

where for conciseness we have written $s = \sin \alpha$ and $c = \cos \alpha$.

For illustrative purposes we now consider the model strain-energy function

$$\Psi = \frac{1}{2}\mu(I_1 - 3) + \frac{k_1}{2k_2}\{\exp[k_2(I_4 - 1)^2] - 1\} + \frac{1}{2}\nu(I^+ - 1)^2 + \frac{1}{2}\nu(I^- - 1)^2 + \frac{1}{2}\kappa(I_8^+ - c_0)^2 + \frac{1}{2}\kappa(I_8^- + c_0)^2. \tag{69}$$

from which it follows that

$$\psi_{I^+} + \psi_{I^-} = 2\nu\gamma[2sc(c_0^2 - s_0^2) + \gamma(s_0^2c^2 + s^2c_0^2)], \tag{70}$$

$$\psi_{I^+} - \psi_{I^-} = 4\nu\gamma s_0 c_0(c^2 - s^2 + \gamma sc), \tag{71}$$

$$\psi_{8+} + \psi_{8-} = 2\kappa\gamma s_0(c^2 - s^2 + \gamma sc), \tag{72}$$

$$\psi_{8+} - \psi_{8-} = 2\kappa\gamma sc_0(2c + \gamma s). \tag{73}$$

Hence, from (68) we obtain

$$\begin{aligned} \sigma_{12} = & \mu\gamma + 2k_1 \exp[k_2\gamma^2 s^2 (2c + \gamma s)^2] s^2 (c + \gamma s)(2c + \gamma s)\gamma + 4v\gamma \{2s^2 c^2 (c_0^2 - s_0^2)^2 + 2s_0^2 c_0^2 (c^2 - s^2)^2 \\ & + 3sc\gamma [(c_0^2 - s_0^2)(c_0^2 s^2 + s_0^2 c^2) + 2s_0^2 c_0^2 (c^2 - s^2)] + \gamma^2 [(c_0^2 s^2 + s_0^2 c^2)^2 + 4s_0^2 c_0^2 s^2 c^2] \} \\ & + 2\kappa\gamma \{s_0^2 + 4s^2 c^2 (c_0^2 - s_0^2) + 3sc\gamma [(s_0^2 c^2 + s^2 c_0^2 + s^2 (c_0^2 - s_0^2))] + 2\gamma^2 s^2 (s_0^2 c^2 + s^2 c_0^2)\}. \end{aligned} \tag{74}$$

In Fig. 7 we plot the dimensionless shear stress $\bar{\sigma}_{12} = \sigma_{12}/\mu$ from (74) against the amount of shear γ in order to illustrate the dependence on the various parameters. Fig. 7(a) shows how the results depend on the angle α_0 of the cross-links relative to the fiber direction for a fixed value of the fiber angle α and each of the other parameters, as specified in the caption.

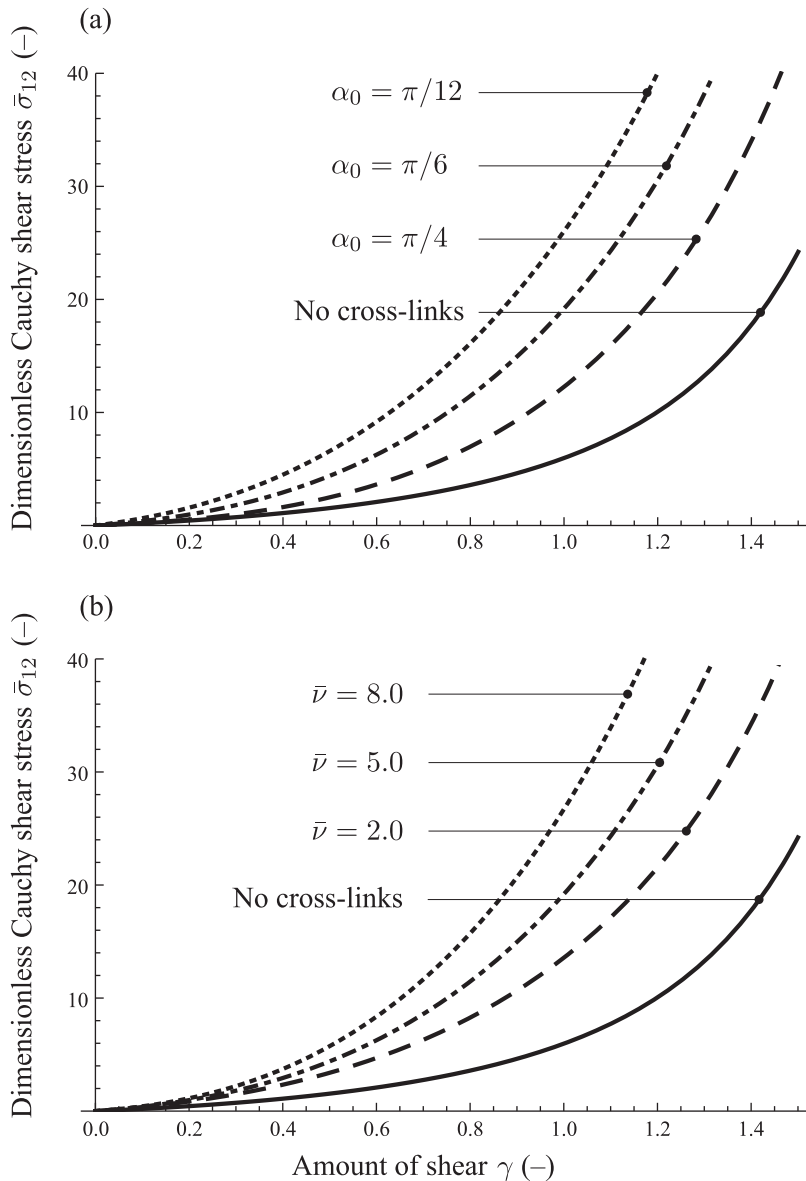


Fig. 7. Plots of the dimensionless Cauchy shear stress $\bar{\sigma}_{12} = \sigma_{12}/\mu$ versus the amount of shear γ : (a) for three values of the cross-link angle α_0 ($\pi/12$, $\pi/6$, $\pi/4$) compared with the plot for the case of no cross-links. On the basis of (74) the following parameters were used: $k_1 = k_1/\mu = 1$, $\bar{v} = v/\mu = 2$, $\bar{\kappa} = \kappa/\mu = 1$, $\alpha = \pi/3$, $k_2 = 0.1$; (b) for four values of the dimensionless cross-link parameter \bar{v} (8.0, 5.0, 2.0, 0). On the basis of (74) the following parameters were used: $\bar{k}_1 = 1$, $\bar{\kappa} = 1$, $\alpha_0 = \pi/6$, $\alpha = \pi/3$, $k_2 = 0.1$.

Analogously to Fig. 4, Fig. 7(b) illustrates the dependence on the density of cross-links via the dimensionless parameter $\bar{\nu}$ and fixed values of each of the other parameters. Once again it is clear that the response becomes stiffer as either the cross-link direction approaches the fiber direction or the density of cross-links increases.

5. Concluding remarks

In this paper we have developed two basic and preliminary continuum models that include the effects of collagen fiber cross-links on the elastic behavior of fibrous soft biological tissues. The first approach is a simple and purely phenomenological extension of a standard model that is used to describe the anisotropic behavior of fibrous tissues by including the dependence on the cross-link density in the anisotropic stiffness parameter of the standard model. This model has been examined for the case of homogeneous simple tension and it illustrates how the stiffness of the material increases with increases in the density of cross-links.

The second model is more general and aims to account for both the relative orientation and stiffnesses of (two families of) collagen fibers and cross-links, and their coupling using an invariant-based strain-energy function. The model is first applied to the case of simple tension in the fiber direction, which shows how the relative orientation of the cross-links and the fibers, and the cross-link stiffness affect the uniaxial response. Then, a more general 3D form with an arbitrary fiber direction and with two symmetrically disposed families of cross-links is provided, which is also suitable for finite element implementation, as needed for solving more complex 3D boundary-value problems. For the purpose of such an implementation, the elasticity tensor for the model in the material description is also provided.

The 2D (plane strain) specialization of the model is applied to the case of a simple shear deformation, and this shows again how the relative orientation of the cross-links and the fibers increases the overall stiffness as the relative orientation is reduced, as well as the cross-link stiffness.

As indicated above, the approaches presented here form initial attempts to incorporate the mechanical properties of cross-links within a continuum model of collagenous soft tissues. This will need further developments as the mechanical properties of cross-links themselves and their interactions with the collagen fibers are determined from experiments, information that is not currently available.

Acknowledgments

The work of G.A.H. was partly supported by the Lead Project on 'Mechanics, Modeling and Simulation of Aortic Dissection', granted by [Graz University of Technology](#), Austria. The work of R.W.O. was in part funded by the UK [EPSRC](#) grant no. [EP/N014642/1](#).

Appendix

The elasticity tensor \mathbb{C} in the material description is defined by

$$\mathbb{C} = 4 \frac{\partial^2 \Psi}{\partial \mathbf{C} \partial \mathbf{C}}. \quad (75)$$

First we introduce some notation and define the following second-order tensors in terms of the basis vectors \mathbf{e}_1 and \mathbf{e}_r , i.e.

$$\mathbf{A}_1 = \mathbf{e}_1 \otimes \mathbf{e}_1, \quad \mathbf{A}_r = \mathbf{e}_r \otimes \mathbf{e}_r, \quad \mathbf{A}_{1r} = \frac{1}{2} (\mathbf{e}_1 \otimes \mathbf{e}_r + \mathbf{e}_r \otimes \mathbf{e}_1) = \mathbf{A}_{r1}. \quad (76)$$

Then, we can write

$$\begin{aligned} \frac{\partial^2 \Psi}{\partial \mathbf{C} \partial \mathbf{C}} = & a_1 \mathbf{I} \otimes \mathbf{I} + a_2 (\mathbf{I} \otimes \mathbf{A}_1 + \mathbf{A}_1 \otimes \mathbf{I}) + a_3 \mathbf{A}_1 \otimes \mathbf{A}_1 + a_4 (\mathbf{I} \otimes \mathbf{A}_r + \mathbf{A}_r \otimes \mathbf{I}) \\ & + a_5 (\mathbf{I} \otimes \mathbf{A}_{1r} + \mathbf{A}_{1r} \otimes \mathbf{I}) + a_6 (\mathbf{A}_1 \otimes \mathbf{A}_r + \mathbf{A}_r \otimes \mathbf{A}_1) + a_7 \mathbf{A}_r \otimes \mathbf{A}_r \\ & + a_8 (\mathbf{A}_1 \otimes \mathbf{A}_{1r} + \mathbf{A}_{1r} \otimes \mathbf{A}_1) + a_9 (\mathbf{A}_r \otimes \mathbf{A}_{1r} + \mathbf{A}_{1r} \otimes \mathbf{A}_r) + a_{10} \mathbf{A}_{1r} \otimes \mathbf{A}_{1r}, \end{aligned} \quad (77)$$

where

$$a_1 = \psi_{11}, \quad a_2 = \psi_{14} + c_0^2 (\psi_{11^+} + \psi_{11^-}) + c_0 (\psi_{18^+} + \psi_{18^-}), \quad (78)$$

$$\begin{aligned} a_3 = & \psi_{44} + 2c_0^2 (\psi_{44^+} + \psi_{44^-}) + c_0^4 (\psi_{11^+} + \psi_{11^-} + 2\psi_{11^-}) + 2c_0 (\psi_{48^+} - \psi_{48^-}) + c_0^2 (\psi_{8^+8^+} + \psi_{8^-8^-} - 2\psi_{8^+8^-}) \\ & + 2c_0^3 (\psi_{1^+8^+} + \psi_{1^-8^+} - \psi_{1^+8^-} - \psi_{1^-8^-}), \end{aligned} \quad (79)$$

$$a_4 = s_0^2 (\psi_{11^+} + \psi_{11^-}), \quad a_5 = s_0 [2c_0 (\psi_{11^+} - \psi_{11^-}) + \psi_{18^+} + \psi_{18^-}], \quad (80)$$

$$a_6 = s_0^2 [\psi_{44^+} + \psi_{44^-} + c_0^2 (\psi_{11^+} + \psi_{11^-} + 2\psi_{11^-}) + c_0 (\psi_{1^+8^+} + \psi_{1^-8^+} - \psi_{1^+8^-} - \psi_{1^-8^-})], \quad (81)$$

$$a_7 = s_0^4 (\psi_{I_1+} + \psi_{I_1-} + 2\psi_{I_1+}), \quad (82)$$

$$a_8 = s_0 [2c_0 (\psi_{4I_1+} - \psi_{4I_1-}) + 2c_0^3 (\psi_{I_1+} - \psi_{I_1-}) + \psi_{48+} + \psi_{48-} + c_0 (\psi_{8+8+} - \psi_{8-8-}) + c_0^2 (3\psi_{I_1+8+} - \psi_{I_1-8+} - \psi_{I_1+8-} + 3\psi_{I_1-8-})], \quad (83)$$

$$a_9 = s_0^3 [2c_0 (\psi_{I_1+} - \psi_{I_1-}) + \psi_{I_1+8+} + \psi_{I_1-8+} + \psi_{I_1+8-} + \psi_{I_1-8-}], \quad (84)$$

$$a_{10} = s_0^2 [4c_0^2 (\psi_{I_1+} + \psi_{I_1-} - 2\psi_{I_1+}) + \psi_{8+8+} + \psi_{8-8-} + 2\psi_{8+8-} + 4c_0 (\psi_{I_1+8+} - \psi_{I_1-8+} + \psi_{I_1+8-} - \psi_{I_1-8-})]. \quad (85)$$

For notational simplicity the indices 1, 4, 8⁺ and 8⁻ in ψ stand for I_1 , I_4 , I_8^+ and I_8^- , respectively, and we have introduced the abbreviation $\psi_{\bullet\bullet} = \partial^2 \Psi / \partial(\bullet) \partial(\bullet)$.

References

- Andriotis, O.G., Desissaire, S., Thurner, P.J., 2018. Collagen fibrils: nature's highly tunable nonlinear springs. *ACS Nano* 12, 3671–3680.
- Barodka, V.M., Joshi, B.L., Berkowitz, D.E., Hogue, C.W., 2011. Review article: implications of vascular aging. *Anesth. Analg.* 112, 1048–1060.
- Buehler, M.J., 2006. Atomistic and continuum modeling of mechanical properties of collagen: elasticity, fracture, and self-assembly. *J. Math. Sci.* 21, 1947–1961.
- Buehler, M.J., 2008. Nanomechanics of collagen fibrils under varying cross-link densities: atomistic and continuum studies. *J. Mech. Behav. Biomed. Mater.* 1, 59–67.
- Cantini, C., Kieffer, P., Corman, B., Limiñana, P., Atkinson, J., Lartaud-Ijdouadiene, I., 2001. Aminoguanidine and aortic wall mechanics, structure, and composition in aged rats. *Hypertension* 38, 943–948.
- Chen, Y.C., Chen, M., Gaffney, E.A., Brown, C.P., 2017. Effect of crosslinking in cartilage-like collagen microstructures. *J. Mech. Behav. Biomed. Mater.* 66, 138–143.
- Davidenko, N., Schuster, C.F., Bax, D.V., Raynal, N., Farndale, R.W., Best, S.M., Cameron, R.E., 2015. Control of crosslinking for tailoring collagen-based scaffolds stability and mechanics. *Acta Biomater.* 25, 131–142.
- Depalle, B., Qin, Z., Shefelbine, S.J., Buehler, M., 2015. Influence of cross-link structure, density and mechanical properties in the mesoscale deformation mechanisms of collagen fibrils. *J. Mech. Behav. Biomed. Mater.* 52, 1–13.
- Eekhoff, J.D., Fang, F., Lake, S.P., 2018. Multiscale mechanical effects of native collagen cross-linking in tendon. *Connect. Tissue Res.* 59, 410–422.
- Eyre, D.R., Paz, M.A., Gallop, P.M., 1984. Cross-linking in collagen and elastin. *Annu. Rev. Biochem.* 53, 717–748.
- Fratzl, P., 2008. *Collagen. Structure and Mechanics.* Springer, New York.
- Fratzl, P., Weinkamer, R., 2007. Nature's hierarchical materials. *Prog. Mater. Sci.* 52, 1263–1334.
- Greenwald, S.E., 2007. Ageing of the conduit arteries. *J. Pathol.* 211, 157–172.
- Hayashi, K., Hirayama, E., 2017. Age-related changes of wall composition and collagen cross-linking in the rat carotid artery – in relation with arterial mechanics. *J. Mech. Behav. Biomed. Mater.* 65, 881–889.
- Holzapfel, G.A., 2000. *Nonlinear solid mechanics. A continuum approach for engineering.* John Wiley & Sons, Chichester.
- Kwansa, A.L., De Vita, R., Freeman, J.W., 2016. Tensile mechanical properties of collagen type I and its enzymatic crosslinks. *Biophys. Chem.* 214–215, 1–10.
- Lin, S., Gu, L., 2015. Influence of crosslink density and stiffness on mechanical properties of type I collagen gel. *Materials (Basel)* 8, 551–560.
- Ogden, R.W., 1997. *Non-linear elastic deformations.* Dover, New York.
- Sáez, P., Peña, E., Martínez, M.A., 2014. A structural approach including the behavior of collagen cross-links to model patient-specific human carotid arteries. *Ann. Biomed. Eng.* 42, 1158–1169.
- Snedeker, J.G., Gautieri, A., 2014. The role of collagen crosslinks in ageing and diabetes - the good, the bad, and the ugly. *Musc. Ligaments Tendons J.* 4, 303–308.
- Spencer, A.J.M., 1984. Constitutive theory for strongly anisotropic solids. In: Spencer, A.J.M. (Ed.), *Continuum Theory of the Mechanics of Fibre-Reinforced Composites.* Springer-Verlag, Wien, pp. 1–32. CISM Courses and Lectures no. 282.
- Svensson, R.B., Mulder, H., Kovanen, V., Magnusson, S.P., 2013. Fracture mechanics of collagen fibrils: influence of natural cross-links. *Biophys. J.* 104, 2476–2484.
- Svensson, R.B., Smith, S.T., Moyer, P.J., Magnusson, S.P., 2018. Effects of maturation and advanced glycation on tensile mechanics of collagen fibrils from rat tail and Achilles tendons. *Acta Biomater.* 70, 270–280.
- Tian, L., Wang, Z., Liu, Y., Eickhoff, J.C., Eliceiri, K.W., Chesler, N.C., 2016. Validation of an arterial constitutive model accounting for collagen content and crosslinking. *Acta Biomater.* 131, 276–287.
- Tsamis, A., Krawiec, J.T., Vorp, D.A., 2013. Elastin and collagen fibre microstructure of the human aorta in ageing and disease: a review. *J. R. Soc. Interface* 10, 20121004.
- Uzel, S.G., Buehler, M.J., 2011. Molecular structure, mechanical behavior and failure mechanism of the C-terminal cross-link domain in type I collagen. *J. Mech. Behav. Biomed. Mater.* 4, 153–161.
- Wagenseil, J.E., Mecham, R.P., 2012. Elastin in large artery stiffness and hypertension. *J. Cardiovasc. Transl. Res.* 5, 264–273.
- Willett, T.L., Labow, R.S., Aldous, I.G., Avery, N.C., Lee, J.M., 2010. Changes in collagen with aging maintain molecular stability after overload: evidence from an in vitro tendon model. *J. Biomech. Eng.* 132, 031002.
- Yang, L., van der Werf, K.O., Dijkstra, P.J., Feijen, J., Binnink, M.L., 2012. Micromechanical analysis of native and cross-linked collagen type I fibrils supports the existence of microfibrils. *J. Mech. Behav. Biomed. Mater.* 6, 148–158.
- Yoshida, K., Jiang, H., Kim, M., Vink, J., Cremers, S., Paik, D., Wapner, R., Mahendroo, M., Myers, K., 2014. Quantitative evaluation of collagen crosslinks and corresponding tensile mechanical properties in mouse cervical tissue during normal pregnancy. *PLoS One* 9, e112391.
- Žagar, G., Onck, P.R., Giessen, E.V.d., 2015. Two fundamental mechanisms govern the stiffening of cross-linked networks. *Biophys. J.* 108, 1470–1479.